Vitis **59**, 9–18 (2020) DOI: 10.5073/vitis.2020.59.9-18

Estimation of grapevine predawn leaf water potential based on hyperspectral reflectance data in Douro wine region

R. Tosin[1), 4)], I. Pôças[1), 2), 3), 4)], I. Gonçalves[5)] and M. Cunha[1), 2), 4)]

[1)] Faculdade de Ciências da Universidade do Porto, Porto, Portugal
[2)] Geo-Space Sciences Research Centre, (CICGE), Porto, Portugal
[3)] Linking Landscape, Environment, Agriculture and Food (LEAF), Instituto Superior de Agronomia, Universidade de Lisboa, Lisboa, Portugal
[4)] Institute for Systems and Computer Engineering, Technology and Science (INESC TEC), Campus da Faculdade de Engenharia da Universidade do Porto, Porto, Portugal
[5)] Associação para o Desenvolvimento da Viticultura Duriense, Edifício Centro de Excelência da Vinha e do Vinho Parque de Ciência e Tecnologia de Vila Real, Régia Douro Park, Portugal

Summary

Hyperspectral data collected through a handheld spectroradiometer (400-1010 nm) were tested for assessing the grapevine predawn leaf water potential (ψ_{pd}) measured by a Scholander chamber in two test sites of Douro wine region. The study was implemented in 2017, being a year with very hot and dry summer, conditions prone to severe water shortage. Three grapevine cultivars, 'Touriga Nacional', 'Touriga Franca' and 'Tinta Barroca' were sampled both in rainfed and irrigated vineyards, with a total of 325 plants assessed in four post-flowering dates. A large set of vegetation indices computed with the hyperspectral data and optimized for the ψ_{pd} values, as well as structural variables, were used as predictors in the model. From a total of 631 possible predictors, four variables were selected based on a stepwise forward procedure and the Wald statistics: irrigation treatment, test site, Anthocyanin Reflectance Index Optimized ($ARI_{opt\_656,647}$) and Normalized Ratio Index ($NRI_{711,700}$). An ordinal logistic regression model was calibrated using 70 % of the dataset randomly selected and the 30 of the remaining observations where used in model validation. The overall model accuracy obtained with the validation dataset was 73.2 %, with the class of ψ_{pd} corresponding to the high-water deficit presenting a positive prediction value of 79.3 %. The accuracy and operability of this predictive model indicates good perspectives for its use in the monitoring of grapevine water status, and to support the irrigation tasks.

K e y w o r d s : handheld spectroradiometer; ordinal logistic regression; spectral vegetation indices; vineyard; grapevine water status.

Introduction

The severe hydric water stress affects the quantity and quality of wine grapes. Therefore, in regions where precipitation is scarce and concentrated in a short period of the year, as in the Mediterranean regions, irrigation has been increasingly considered to regulate grapevine yield and quality (e.g. Chaves *et al.* 2010). An example of this increasing irrigation trend can be observed in Douro wine region, a worldwide known wine region (Cunha and Richter 2016). However, in the context of foreseen warming and dry climate scenarios and the increasing competition for water among different economic sectors, a correct irrigation management is essential to ensure the sustainability of Mediterranean irrigated areas (Cunha and Richter 2016, Medrano *et al.* 2015).

The grapevine irrigation scheduling is often based on ecophysiological measures of vine water status. One of the most widely used measures is referred to the predawn leaf water potential (ψ_{pd}) using a Scholander chamber (Scholander *et al.* 1965). Despite being a very reliable technique (Moutinho-Pereira *et al.* 2007, Merli *et al.* 2015, Alves *et al.* 2012), it is a destructive method (Rodríguez-Pérez *et al.* 2018) and depends on the collection of a large set of measurement points to get a very accurate assessment of the target area due to the variability in soil conditions (Oumar and Mutanga 2010). Thus, efforts have been made to find alternative methods capable of providing accurate information about vine water status, while being easy-to use and non-destructive.

The contribution of remote sensing to improve water management has increased in recent years. Spectral reflectance obtained through proximity sensors (e.g. handheld spectroradiometers), cameras mounted on drones or satellite imagery has been widely used to estimate and map crop biophysical parameters (Zarco-Tejada *et al.* 2013, Blackburn 2007), including for estimating and monitoring water status in vineyards (Pôças *et al.* 2015 and 2017, Rodríguez-Pérez *et al.* 2018). Different zones of the electromagnetic spectrum have been studied for the monitoring of plant water status, including near and mid infrared, which present wavelengths of strong water absorption of the radiation, and the shortwave infrared due to the relation between canopy temperature and crop water status (Bellvert *et al.* 2014, Clevers *et al.* 2010). Additionally,

Correspondence to: Dr. M. Cunha, Faculdade de Ciências da Universidade do Porto, Rua do Campo Alegre, Porto 4169-007, Portugal. E-mail: mccunha@fc.up.pt

the spectral zones of visible and near infrared (NIR) are potentially useful to estimate crop water status (Suárez *et al.* 2008, De Bei *et al.* 2011). Additionally, the spectral data from the visible and NIR domains are more easily accessible from commonly available handheld spectroradiometers, as well as from sensors mounted on satellite and/or unmanned aerial vehicles (Zarco-Tejada *et al.* 2013).

A particular focus for assessing crop water status has been given to the use of hyperspectral vegetation reflection data, which are characterized from numerous narrow bands continuously distributed across the electromagnetic spectrum. These hyperspectral data are sensitive to subtle variations in the energy reflected and thus have great potential for detecting differences between vegetation characteristics (Blackburn 2007, Jones and Vaughan 2010, Mariotto *et al.* 2013). Nevertheless, the large amount of data generated from hyperspectral sensors can result in redundancy of the information captured (Blackburn 2007, Wu *et al.* 2008, Caicedo *et al.* 2014, Rivera *et al.* 2014, Feng *et al.* 2017). Thus, the adequate data processing, coping with dimensionality issues, wavelengths selection and modelling tools are required for its efficient use.

The hyperspectral reflectance data can be combined into vegetation indices (VI) frequently at two or three wavelengths, which can be specifically optimized for vines water status, and thus only using a small portion of the spectrum (Suárez *et al.* 2008, Zarco-Tejada *et al.* 2013, Pôças *et al.* 2015). There is a large set of VI related to structural, biochemical, and physiological parameters of the vegetation as reported in the literature (Jones and Vaughan 2010, Roberts *et al.* 2012). The Normalized Difference Vegetation Index (NDVI) (Tucker 1979), the Soil-Adjusted Vegetation Index (SAVI) (Huete 1988) and the Enhanced Vegetation Index (EVI) (Huete *et al.* 1997) are among the most frequently used VI, being particularly useful to assess parameters related to the vegetation status and structure. Additionally, some VI have been specifically designed to estimate parameters, such as the leaf water content and Chlorophyll concentration. Examples of such indices include the Potential Water Index (PWI) (Peñuelas *et al.* 1997) and the Photochemical Reflectance Index (PRI) (Gamon *et al.* 1992), respectively.

Recently, the techniques of machine learning have been used to cope with the high dimensionality of hyperspectral datasets. Several studies have applied non-parametric regression models to estimate the water status in grapevines, (Pôças *et al.* 2017, Rodríguez-Pérez *et al.* 2018). The machine learning classification methods have also been applied to hyperspectral data for estimating biophysical and biochemical crop parameters (Im *et al.* 2009). One of such classification methods is the ordinal logistic regression (OLR), which is used to explain a ranking variable (Harrell 2015), and has been employed in many environmental studies (Brant 1990, Rutherford *et al.* 2007, Coppock 2011, Notario del Pino and Ruiz-Gallardo 2015). The OLR algorithm has been used for modelling the relationship between an ordinal response variable and one or several continuous independent variables, while considering the inherent ordering of the response variable, thus making full use of the ordinal information (Kleinbaum and Klein 2010). Often, the OLR is fitted through a proportional-odds logit model (McCullagh 1980), applied to obtain an ordinal response (Verwaeren et *al.* 2012). The proportional-odds logit model assumes that identical feature variables might result in different values for the underlying response variable and therefore the model contains a deterministic component and an error term, which is assumed to follow a logistic distribution (Verwaeren *et al.* 2012).

Although the ψ_{pd} obtained with pressure chamber (e.g. Sholander chamber) is recorded as a continuous variable, farmers often use classes of ψ_{pd} to characterize the water status in grapevines in order to support irrigation decisions (Deloire *et al.* 2005). Therefore, we argue that machine learning classification methods based on hyperspectral data could be an alternative to estimate grapevine ψ_{pd}, resulting classes of water status. Thus, the main goal of this work is modelling the water status in grapevines through a classification predictive regression model based on hyperspectral data. Specific goals include testing and validating the model in two different zones of Douro Wine region and considering three cultivars growing under two irrigation regimes.

Material and Methods

Study area: This study was conducted in the Douro Wine Region, Northeast of Portugal (Fig. 1), where 45,613 ha of vineyards dominate the landscape and are established mainly over terraces and slopes with shale-derived soils (IVDP 2018). The Douro region is recognized worldwide, both by its classification as UNESCO World Heritage Cultural Landscape and by the exquisite quality of the Porto wine here produced. The region is divided into three sub-regions: Baixo Corgo (vineyard area of 14,582 ha), Cima Corgo (vineyard area of 20,969 ha), and Douro Superior (vineyard area of 10,175 ha), distributed from the western up to eastern part of the region (Fig. 1), all with rigorous climate conditions.

The Douro wine region is one of the most arid regions of Europe where a strong water stress occurs in summer as a consequence of the low soil water content, associated

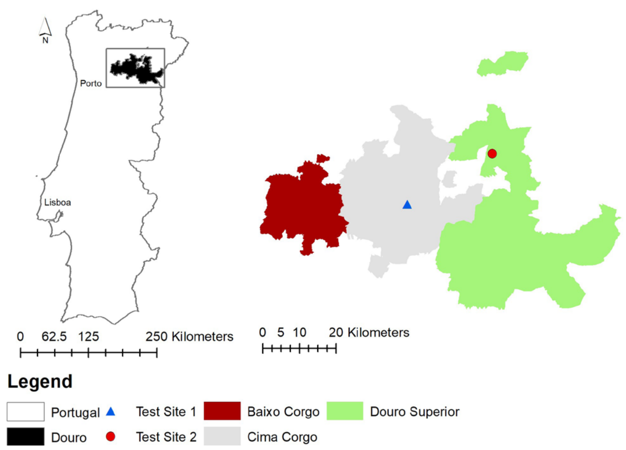

Fig. 1: Location of the study area, identifying the test sites 1 and 2 in the Douro Wine Region, Northeast Portugal, and the respective sub-regions: Baixo Corgo, Cima Corgo and Douro Superior.

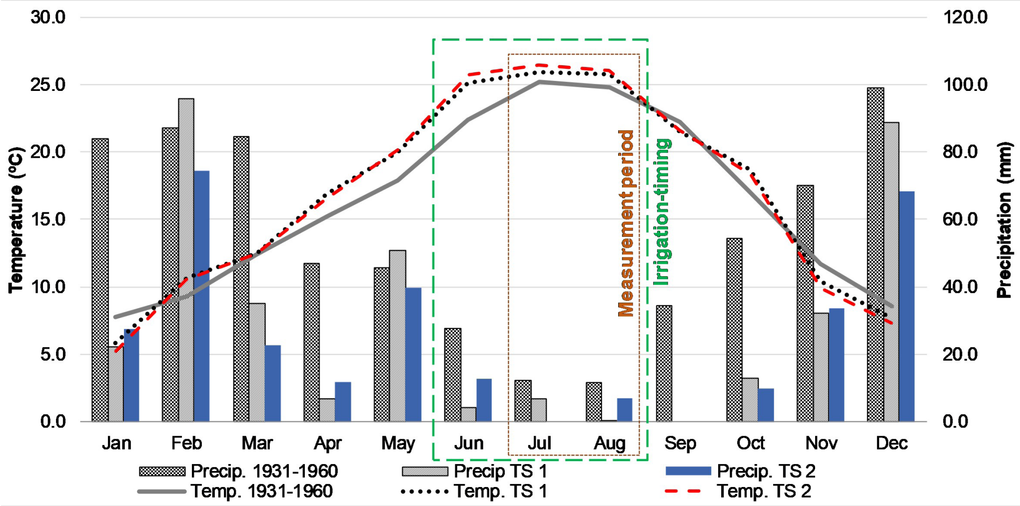

Fig. 2: Temperature and precipitation characterization of the Douro wine region for the reference period 1931-1960 (Ferreira 1965) and comparison with the temperature and precipitation records in 2017 during study period in the test site 1 (TS 1) and test site 2 (TS 2). The irrigation-timing and measurement period are highlighted in the figure.

to the low annual rainfall and high gradients of the water vapour pressure between the leaves and the air (Jones and Alves 2012, Alves *et al.* 2013, Prata-Sena *et al.* 2018). The region has a Mediterranean climate, with high average temperatures during the summer period, ranging between 22.4 °C in Baixo Corgo and 24.1 °C in Douro Superior and Cima Corgo (INMG 1991). In Baixo Corgo the annual precipitation is 856 mm, while in Cima Corgo it is 658 mm and in Douro Superior it is 539 m, with summer precipitation representing 10.3 %, 8.8 % and 7.4 % of the annual precipitation, respectively. A detailed characterization of the region and sub-region climate is presented by Pôças *et al.* (2017). Fig. 2 compares the climate characterization of the Douro Wine Region in both test sites in the year 2017.

Two commercial vineyards were considered for the study (Fig. 1): (i) Test site 1 (TS1) – Quinta dos Aciprestes (wine company Real Companhia Velha) located in Cima Corgo sub-region (Latitude 41.21°N; Longitude 7.43°W; 145 m a.s.l.), and (ii) Test site 2 (TS2) – Quinta do Ataíde (wine company Symington), in Douro Superior (Latitude 41.25°N; Longitude 7.11°W; m a.s.l.).

In test site 1 the cultivars studied were: (i) Touriga Nacional (TN) – two plots, with two replicate areas, including three irrigation treatments: non-irrigated (TN_NI), irrigation treatment 1 (TN_IT1), and irrigation treatment 2 (TN_IT2), and (ii) Touriga Franca (TF) – a single plot and a single treatment (TF_IT). Three cultivars were studied in test site 2: (i) TN – two plots (TN1 and TN2) with two irrigation treatments: irrigated (TN1_IT, TN2_IT) and non-irrigated (TN1_NI, TN2_NI), (ii) TF – one plot with an irrigated treatment (TF_IT) and a non-irrigated treatment (TF_NI), and (iii) Tinta Barroca (TB) – one plot with an irrigated treatment (TB_IT).

The vines pruning system is Bilateral *Royat* in both test sites with planting spacing and vines maximum height respectively of 2.2 m ×1 m and 1.5 m in test site 1 and 2.1 m ×1.1 m and 1.8 m in test site 2.

The irrigation scheduling and the irrigation amounts were managed by each wine company, based on information of ψ_{pd} regular measurements and aiming to adjust for quality criteria. Tab. 1 summarizes the irrigation dates and amounts in each test site.

In both test sites, the total irrigation amount in TN is greater than that applied in TF (up to 25 %). TB is the grape variety that received the highest amount of irrigation (137.6 L·plant^{-1}).

Ground measurements: The study was conducted in 2017 between post-flowering (end of June) and the harvest (early September). During this period, the average temperature was 24.6 °C in the test site 1 and 25 °C in the test site 2 and the precipitation in test site 1 was 11.2 mm while for test site 2 it was 19.6 mm (Fig. 2). The year 2017 was characterized by high temperatures and extremely low precipitation during the summer period, forcing producers to pick earlier in both test sites.

Ground measurements of ψ_{pd} data and spectral reflectance data were collected at four dates in both test sites: test site 1 (July 5, July 20, August 3, and August 31) and test site 2 (July 4, July 21, August 4, and September 1). A minimum of six plants per irrigation treatment and plot were sampled in each test site for ground measurements, resulting in 325 observations (grapevines), 135 in test site 1 and in test site 2 (Tab. 2).

A pressure chamber (Scholander *et al.* 1965) (PMS600, Albany, OR, USA) was used for measuring the ψ_{pd}. The measurements were done at predawn, around 6 AM, on one leaf from each vine per block sampled. A large variability both between test sites and within each test site was recorded in the ψ_{pd} dataset.

The hyperspectral data were measured using a portable spectroradiometer (Handheld 2, ASD Instruments, Boulder, CO, USA), with a field-of-view of 25°, a spectral resolution < 3 nm at 700 nm, a wavelength accuracy of ± 1 nm. During measurements, the equipment was maintained approximately 30 cm above canopy, which gives a sampling footprint of approximately 13.3 cm. Measurements over a white spectralon panel, also called white reference standard, were done prior to measurements over the target plants aiming to calibrate the level of reflectance. The

Table 1

Irrigation dates and irrigation amounts (L/Plant/day) per test site and irrigation treatment. Test site 1: TN_IT1 – 'Touriga Nacional' – irrigation treatment 1; TN_IT2 – 'Touriga Nacional' – irrigation treatment 2; TF_IT – 'Touriga Franca' – irrigation treatment. Test site 2: TN1_IT – 'Touriga Nacional', plot 1 – irrigation treatment; TN2_IT – 'Touriga Nacional', plot 177 2 – irrigation treatment; TF_IT – 'Touriga Franca' – irrigation treatment; TB_IT – 'Tinta Barroca' – irrigation treatment

Date	Test site 1*			Date	Test site 2*			
	TN_IT1	TN_IT2	TF_IT		TN1_IT	TN2_IT	TF_IT	TB_IT
19 June	16	16	16	20 June	9.6	9.6		16
23 June	0	16	0	24 June	16	16	16	16
29 June	16	16	16	1 July	19.2	19.2	16	19.2
13 July	16	16	16	7 July	19.2	19.2	16	19.2
21 July	16	16	16	15 July	16	16	16	19.2
28 July	16	16	16	25 July	16	16	16	16
4 August	0	16	0	31 July	16	16	16	16
11 August	12	12	12	7 August	16	16	16	16
				14 August	16	16	13	16
				22 August	13	13		
Total	92	124	92		128	128	112	137.6

*Drip irrigation system with emitters discharge: Test site 1: 2 Lh-1; Test site 2: 1.6 Lh-1 with spacing between emitters of 1 m (test site 1) and 0.5 m (test site 2).

Table 2

Number of observations (gapevines) per test site, cultivar and irrigation conditions

Test site	Cultivar	Irrigated	Non-irrigated	Total
Test site 1	Touriga Nacional	64	31	95
	Touriga Franca	40	0	40
Total Test site 1		104	31	135
Test site 2	Touriga Nacional	68	68	136
	Touriga Franca	18	18	36
	Tinta Barroca	18	0	18
Total Test site 2		104	86	190
Total		208	117	325

spectroradiometer records reflectance signatures between 325 nm and 1075 nm of the electromagnetic spectrum (corresponding to visible and NIR), with a wavelength interval of 1 nm. However, only reflectance data between 400 nm to 1010 nm were considered due to noise occurrence outside of these spectral limits. The measurements were done in cloud free days between 11 h to 14 h (local time) to minimize changes in solar zenith angle. Ten repetitions per plant were collected and later averaged to minimize the effect of noise.

Data processing: The hyperspectral and ψ_{pd} data were analyzed by each plant (Tab. 2). A one-way analysis of variance (ANOVA) with *p*-value associated to the Fischer test was performed to compare the means of ψ_{pd} between the test sites regarding the 12 irrigation treatment and the cultivars. These statistical analysis were computed in R (R Core Team 2017) combined with car package (Fox and Weisberg 2011) and agricolae package (Mendiburu 2017). The hyperspectral data were processed into spectral vegetation indices (VI). A large 222 diversity of VI, including two-band indices, represented by simple ratios (SR), normalized indices (NRI) and also other formulations defined in the literature were computed (Tab. 3).

Following previous studies (Pôças *et al.* 2015 and 2017), a band selection procedure for the two-band vegetation indices optimization was considered, testing all two-band combinations (for simple ratio indices and normalized indices) within the spectral range of 400 nm and 1010 nm. Additionally, all combinations of bands for smaller sub regions of the spectrum (spectral domains) were tested for the normalized difference vegetation index formulation. In this last case, all combination of bands within specific combinations of the spectral domains of blue, green, red, red edge, and near infrared were tested. The range considered for each spectral domain was 451-520 nm for blue, 521-570 nm, for green, 571-700 nm for red, 681-740 nm for red edge, and 701-950 nm for near infrared (NIR). A linear fitting function was used for the band selection opti-

Table 3

Vegetation indices formulations with bands (b) optimized according to grapevines predawn leaf water potential

Vegetation index[a]	Formulation	Original reference
2-bands - Normalized indices		
$NRI_{515,523}$	$NRI_{515,523} = (b_{523} - b_{515})/(b_{523} + b_{515})$	-
$NRI_{520,701}$	$NRI_{520,701} = (b_{520} - b_{701})/(b_{520} + b_{701})$	-
$NRI_{520,615}$	$NRI_{520,615} = (b_{520} - b_{615})/(b_{520} + b_{615})$	-
$NRI_{520,694}$	$NRI_{520,694} = (b_{520} - b_{694})/(b_{520} + b_{694})$	-
$NRI_{524,615}$	$NRI_{524,615} = (b_{524} - b_{615})/(b_{524} + b_{615})$	-
$NRI_{535,701}$	$NRI_{535,701} = (b_{535} - b_{701})/(b_{535} + b_{701})$	-
$NRI_{529,694}$	$NRI_{529,694} = (b_{529} - b_{700})/(b_{529} + b_{700})$	-
$NRI_{711,700}$	$NRI_{711,700} = (b_{711} - b_{700})/(b_{711} + b_{700})$	-
$NRI_{718,723}$	$NRI_{718,723} = (b_{718} - b_{723})/(b_{718} + b_{723})$	-
2-bands - Simple ratios		
$SR_{718,723}$[a]	$SR_{718,723} = b_{723}/b_{718}$	-
$WI_{900,970}$	$WI_{900,970} = b_{900}/b_{970}$	(Peñuelas *et al.* 1993)
2-bands - Other formulations		
$ARI_{opt\_665,647}$	$ARI_{opt\_665,647} = (1/b_{647}) - (1/b_{665})$	(Gitelson *et al.* 2001b)
$MSAVI_{opt\_701,587}$	$MSAVI_{opt\_701,587} = [2 * b_{701} + 1 - [(2 * b_{701} + 1)^2 - 8(b_{701} - b_{587})]^{½}]/2$	(Qi *et al.* 1994)
$OSAVI_{opt\_745,700}$	$OSAVI_{opt\_745,700} = (b_{745} - b_{700})/(b_{745} + b_{700} + 0.16$	(Rondeaux *et al.* 1996)
$RDVI_{opt\_745,700}$	$RDVI_{opt\_745,700} = (b_{745} - b_{700})/[(b_{745} + b_{700})^{½}]$	(Roujean and Breon 1995)

[a] NRI - Normalized Reflectance Index; SR – simple ratio; WI – Water Index; ARI_{opt} – Anthocyanin Reflectance Index optimized; $OSAVI_{opt}$ - Optimal Soil Adjusted Vegetation Index optimized; $MSAVI_{opt}$ - Modified Soil Adjusted Vegetation Index optimized; $RDVI_{opt}$ - Renormalized Difference Vegetation Index optimized.

mization, having the ψ_{pd} as the dependent variable. A calibration dataset, corresponding to 70 % of the total observations, and a validation dataset, with the 30 % remaining observations, were used for assessing the best combination of bands. The bands selected for each VI corresponded to the best combinations obtained for both the calibration and validation datasets, expressed through the determination coefficient (R^2). A total of fifteen VI were selected following the optimization procedure (Tab. 3).

The VI computation and bands optimization were performed in the HSDAR package (Lehnert *et al.* 2017), implemented in software R (R Core Team 2017) and in the spectral indices toolbox of Automated Radiative Transfer Models Operator (ARTMO) software (Verrelst *et al.* 2011, Rivera *et al.* 2014).

A time-dynamic variable based on the ψ_{pd} (ψ_{pd_0}) was also used as predictor aimed at representing crop water status dynamics in the post-flowering - harvest period. This variable is aimed at minimizing the spurious downward time trend inherent to both ψ_{pd} and hyperspectral data. The time trend effect was discussed by Pôças *et al.* (2017). This ψ_{pd_0} was computed by integrating, in each measurement date to be predicted, the information of previous ψ_{pd} measurements. The ψ_{pd_0} was defined for each measurement point and measurement date as the ψ_{pd} value corresponding to the previous measurement. For the first measurement date (test site 2: July 4th; test site 1: July 5th), a presumed value based on expert knowledge, was considered, corresponding to 70 % of the ψ_{pd} measured in each point.

Modelling approaches: In the modelling approaches the ψ_{pd} was used as response variable and 631 predictor candidates were considered. These potential predictors originated from both hyperspectral (626) and structural (5) data. The potential predictors relative to hyperspectral data were: i) spectral reflectance of 611 wavelengths in the range between 400 nm and 1010 nm (wavelength interval of 1 nm), ii) 15 vegetation indices (Tab. 3). The potential predictors relative to structural parameters included: i) irrigation conditions (two levels: IT_I – irrigated, IT_NI – non-irrigated), ii) cultivar (tree levels: TN, TF, and TB), iii) test site (two levels: TS_1 and TS_2), iv) the time-dynamic predictor ψ_{pd_0} (three levels of the 15 classification: ψ_{pd_0-1}: low ψ_{pd_0-2}: moderate, and ψ_{pd_0-3}: high) and v) the days after flowering (DAF).

To run the statistical model, the dataset was split into training data (70 % of random observations) and validation data (30 % of the remaining observations) (Kuhn and Johnson 2013). The training and validation datasets integrate the pairs of concurrent measurements of the ψ_{pd} and the corresponding values of the predicting variables.

A stepwise regression procedure was used for selection within the initial 631 predictor candidates. Following this procedure, the predicting variable that most contributes to the model improvement in each step, compared to the model in the previous step, is chosen based on the lowest value of Akaike information criterion (AIC; Akaike (1974). The AIC is based on the maximum likelihood function allowing the comparison of models with different number of predictors.

This algorithm is based on the number of observations in the model (N), the sum of square error (SQE), and the number of parameters +1 (K), according to equation (1) (Akaike 1974, Burnham 2002).

$$AIC = Nxln\left(\frac{SQE}{N}\right) + 2k$$

In the modelling approach, the ψ_{pd} was used as categorical variable. The definition of classes of ψ_{pd} values was based on the analysis of the ψ_{pd} dispersion and on the ψ_{pd} threshold of -0.5 MPa often considered by farmers in Mediterranean regions for irrigation decisions under deficit irrigation strategies (Van Leeuwen *et al.* 2009, Lopes *et al.* 2011). Three class labels were defined: (i) class 1 (low water deficit): 0 MPa > ψ_{pd} ≥ -0.25 MPa; (ii) class 2 (moderate water deficit): -0.25 MPa > ψ_{pd} ≥ -0.5 MPa; and (iii) class 3 (high water deficit): 291 -0.5 MPa > ψ_{pd}.

Predictive modelling applied in classification mode: The OLR was selected for modeling the ordinal response variables ψ_{pd}. The OLR allows building a predictive model on a probabilistic basis. In the present study, the OLR was fitted through a proportional-odds logit model (McCullagh 1980), which is widely applied to represent ordinal responses (Verwaeren *et al.* 2012). The proportional-odds logit model defines a probability density function over the class labels for a given feature vector x, which belongs to the input space X (McCullagh 1980, Verwaeren *et al.* 2012).

The "polr" function from the MASS library in software R (Venables and Ripley 2002) was used for (Harrell Jr. 2018) applying this methodological approach.

Model performance assessment: The residual deviance (McCullagh, 1980, Kleinbaum and Klein 2010) and the Akaike information criterion (AIC; Akaike (1974)) were computed for assessing the model's quality. The AIC statistics allows comparing between model's performance, with lower AIC values corresponding to simpler models with fewer predictors (Kuhn and Johnson 2013). The Wald statistic was also used to assess the significance of the predictors selected for the model (Peng *et al.* 2002). The odds ratios were calculated to analyse the weight of each predictor. Additionally, the positive prediction value by class and the overall model accuracy were computed and organized in a confusion matrix. The overall model accuracy corresponds to the agreement between predicted and observed values in each categorical class, making no distinction in the types of misclassification (Kuhn and Johnson 2013). The calculated positive prediction value reports the percentage of correct classification cases by class considering the prevalence of the event (Kuhn and Johnson 2013). The caret package (Kuhn 2018), implemented in software R (R Core Team 2017), was used to automatically compute the confusion matrices resulting from the predictive modelling approach in the classification mode.

Results

Analysis of the variability between and within test sites: The impact of irrigation treatments and cultivars in each test site on the ψ_{pd} is presented in Tab. 4. The test site 2 consistently presented lower ψ_{pd} values (Fig. 3), evidencing that vineyards in this test site of sub-region of Douro Superior (Fig. 2) are more likely to present higher water deficit conditions. In both test sites, the irrigation and the grapes varieties presented a significant impact on ψ_{pd} values.

The TF present higher ψ_{pd} in both test sites, even with lower irrigation amounts (Tab. 1), may be an indicator of better water use efficiency due to the lower amount of water required and higher ψ_{pd} when compared to TN (Tab. 4). Nevertheless, it is important to highlight that only in the test site 1 the ψ_{pd} values are statically different (TN). Although the TB recorded higher mean values of ψ_{pd}, this cannot reflect a better water use efficiency of this grape variety, since it also received higher amounts of irrigation (Tab. 1). The maintenance of this high ψ_{pd} in TB, associated to high irrigation amounts, can be justified by the high sensitivity (yield and quality) of this grape variety to water stress (IVV 2011).

Model performance: Tab. 5 presents the statistics of the coefficients included in predictive models (model 1 and model 2) developed for assessing the grapevine ψ_{pd}. From the potential predictors initially considered, only nine were selected through the stepwise procedure: i) two qualitative variables: Irrigation treatment (IT) and Test site (TS); ii) four vegetation indices: $ARI_{opt\_656,647}$, $NRI_{745,700}$, $NRI_{711,700}$, $WI_{900,970}$; iii) days after flowering (DAF); iv) ψ_{pd_0}, and iv) one wavelength: R996. Then, the OLR model was applied to these nine predict-

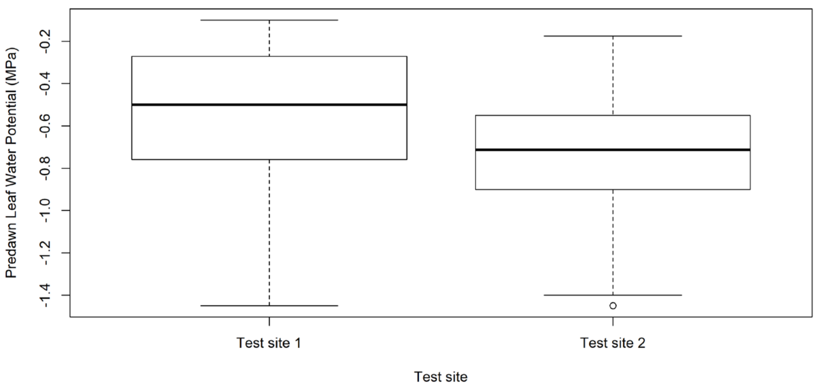

Fig. 3: Dispersion of predawn leaf water potential (MPa), represented by a boxplot for the test site.

Table 4

Statistical results of mean predawn leaf water potential (ψ_{pd}, MPa) for the different irrigation regimes and grape varieties in the test sites studied

Structural parameters	N. Obs	Location (ψ_{pd}, MPa)		Mean ψ_{pd} (MPa)	ANOVA *p*-value*
		Test site 1	Test site 2		
Irrigation					
- No irrigation	117	-0.822	-0.976	-0.936	0.002
- Irrigation	208	-0.434	-0.559	-0.496	0.000
ANOVA F*		0.000	0.000	0.000	---
Grape cultivars					
T. Nacional (TN)	231	-0.566^{b}	-0.781^{b}	-0.692^{b}	0.000
T. Franca (TF)	76	-0.423^{a}	-0.726^{b}	-0.566^{ab}	0.000
T. Barroca (TB)	18	na	-0.541^{a}	-0.541^{a}	---
ANOVA F*		0.012	0.003	0.003	---
Overall mean	325	-0.523	-0.748	-0.655	0.000

ANOVA *p*-value*: is the *p*-value associated to Fischer's test performed in the ANOVA; means with *p*-value less than 0.05 is considered statistically different. Within columns, means followed by the same letter are not significantly different according to Duncan's test ($\alpha < 5$ %). na: no data available

Table 5

Coefficients determinate by Wald Statistics and odd ratios of the predictors in the models developed to estimated ψ_{pd}

Predictors	Model 1		Model 2	
	Coefficient	Odd ratio	Coefficient	Odd ratio
IT_NI	3.06 x 10***	1.95×10^{13}***	1.89 x 10***	1.68×10^{8}***
Test site_2	1.10***	3.01***	1.35***	3.86***
$ARI_{opt\_656,647}$	1.92***	6.83***	1.77***	5.86***
DAF	-4×10^{-3}	9.96×10^{-1}	-	-
$NRI_{745,700}$	-1.43	2.40×10^{-1}	-	-
$NRI_{711,700}$	-2.28 x 10***	0.00***	-1.80 x 10***	0.00***
$WI_{900,970}$	9.13	9.26×10^{3}	-	-
ψ_{pd_0}	3.63×10^{-1}	1.44	-	-
R996	-2.05	$1.28*10^{-1}$	-	-

IT_NI: non-irrigation treatment; TS_2: Test site 2; $ARI_{opt\_656,647}$: Anthocyanin Reflectance Index optimized; DAF: days after flowering; NRI: Normalized reflectance index; WI: Water index; R996: reflectance at wavelength 966 nm. ψ_{pd_0}: time-dynamic variable based on ψ_{pd} of the previous measurements; *$p < 0.1$; **$p < 0.05$; ***$p < 0.01$.

ing variables selected by the stepwise method (model 1, Tab. 5). This model 1 presented an AIC value of 270.88.

The results of the individual regression coefficients of Wald statistics for each predictor, showed that only the variables "IT_NI", "TS_2", "$ARI_{opt\_656,647}$" and "$NRI_{711,700}$" were statistically significant ($p < 0.01$) (Tab. 5). These results suggest that an alternative model (model 2) including these four statistically significant predictors could be applied to the data. The model 2, combining the four selected variables, presents AIC of 262.06. This AIC value improved when compared to model 1. For the model 2 the results of the odds ratio indicate that the non-irrigation treatment (IT_NI) has the biggest influence on the assignment of the class, followed by the $ARI_{opt\_656,647}$, test site 2 (TS_2), and the $NRI_{711,700}$. The model 2 overall accuracy, assessed through the validation dataset, was 73.2 % and the positive prediction value per class was 33.3 %, 44.4 % and 79.3 %, respectively, for the classes low (1), moderate (2), and high (3) water deficit (Tab. 6). The variability in the prediction value per class is likely due to the impact of the imbalanced data set used for validation (10, 20 and 67 cases in class 1, class 2, and class 3, respectively).

Table 6

Confusion matrix for the comparison between observed and predicted predawn leaf water potential (ψ_{pd}) in the validation dataset (97 observations; 30 % of the dataset)

ψ_{pd} predicted	ψ_{pd} observed Low	Moderate	High	Positive prediction by class (%)
Low	2	3	0	33.3%
Moderate	5	6	2	44.4 %
High	3	11	65	79.3 %

Predawn leaf water potential (ψ_{pd}) classes: low water deficit, 0 MPa > ψ_{pd} > -0.25 MPa; moderate water deficit, -0.25 MPa > ψ_{pd} > -0.50 MPa; high water deficit, <-0.50 MPa.

Discussion

The hyperspectral based predictive model developed is a valuable tool for predicting grapevine ψ_{pd} because of the integration of variables relative to agronomic practices (Irrigation Treatment, IT) and ecological conditions of grape-growth (Test Site, TS), as well as proxies of biophysical features (expressed by the optimized vegetation indices $ARI_{opt\_656,647}$ and $NRI_{711,700}$).

The selection of a predictor related with the IT is consistent with the differences between irrigation treatment (Tab. 4) resulting in differences on the reflectance of irrigated and non-irrigated plants (Pôças *et al.* 2017). The selection of a variable relative to the test site is likely associated to the different climatic conditions between sub-regions of Douro wine region (Fig. 2), with the test site 2 located in a usually warmer and drier zone than test site 1. Both irrigation and test site variables will influence the canopy reflectance, that will be expressed in the ψ_{pd} values and consequently in the VI calculated. The selection of these 22 variables allows to see how different the canopy behaves under different climatic conditions and the band combination expressed in the VI works as proxy of the vegetation status.

Following the VI optimization for bands selection, the proposed $ARI_{opt\_656,647}$ integrates wavelengths of the red spectral domain, close to the red edge domain, instead of the wavelengths of the original formulation in the green and the red edge domains (Gitelson *et al.* 2001a). The wavelengths of $ARI_{opt\_656,647}$ are close to those studied by Blackburn (2010), the wavelengths of 680 nm and 635 nm, which are related to the chlorophyll a and chlorophyll b concentrations, respectively. Also, Sonobe *et al.* (2018) studied similar bands range to estimate the chlorophyll content. The content of chlorophylls a and b is a potential indicator of vegetation stress (Zarco-Tejada *et al.* 2002, Wu *et al.* 2008), which includes water stress. As discussed by these authors, several physiological perturbations in the light-dependent reactions of photosynthesis that occur in plants under stress can be related with changes in chlorophylls a and b, and assessed through differences in spectral reflectance. The $NRI_{711,700}$ combines wavelengths of red and red edge. The red-edge zone is reported as a potential indicator of water stress in plants and thus the construction of VI using this zone of the spectrum can provide information about the crop water status (Zarco-Tejada *et al.* 2013, Fang *et al.* 2017, Rodríguez-Pérez *et al.* 2018).

Also other studies have used optimized VI combined with modelling approaches to assess biophysical variables related with water status in different crop types (e.g. Rallo *et al.* (2014), Pôças *et al.* (2017).

As discussed in previous studies, the spectral information, and specifically the optimized VI, can work as proxy of biophysical variables (Zarco-Tejada *et al.* 2013, Rallo *et al.* 2014). The results obtained in the present study are consistent with the findings by Maimaitiyiming *et al.* (2017), who reported that stomata conductance (a water status 23 indicator) can be related to spectral bands close to those selected in our study for the optimized VI. Additionally, those authors reported that stomata conductance is strongly related to indicators of chlorophyll content.

Although a good accuracy of prediction (73.2 %) was obtained, the model was able to better classify the classes of higher stress, which may be due to the imbalanced number of observations of each class in the data set. As discussed by Brodersen *et al.* (2010), an imbalanced data set may lead to misleading conclusions about the performance of a classification predictive model when using an average accuracy measure.

The analysis of the positive prediction frequency per class, shows a good performance (79.27 % of cases correctly classified) for the class of high-water deficit (class 3; ψ_{pd} < -0.5 MPa). In Mediterranean regions, where the grapevine is frequently conducted under deficit irrigation strategies the irrigation schedule often starts when plants are under ψ_{pd} values below -0.5 MPa (Van Leeuwen *et al.* 2009, Lopes *et al.* 2011). Therefore, the good results obtained for this specific class of ψ_{pd} are particularly interesting to support grapevine deficit irrigation strategies, aimed at promoting grape quality, which are generally implemented in the most technologically advanced grape-growers.

Conclusion

In this study we presented how the ψ_{pd} in vineyards of Douro wine region could be predicted by a classification model based on hyperspectral reflectance data. A large set of climatic, environmental, and agronomic conditions were sampled to test model's accuracy and robustness. The developed predictive model presented an overall accuracy of 73.2 %. The variables selected provide information of plant physiology relevant for the prediction of the water status in grapevines. Nevertheless, the modelling could be improved if a higher number of samples were assessed in the field to avoid problems related to imbalanced observations in the classes.

The use of the classification model to estimate ψ_{pd} brings a potential application to support irrigation decision in viticulture. Usually, the operational decisions about the vine's irrigation scheduling are done for ψ_{pd} values associated to the class 3 of this study, where the model obtained good performance. Therefore, the results of the proposed model have potential to be used in support to irrigation tasks. Moreover, the use of classes of ψ_{pd} instead of continuous values provides easier-to-use information for farmers. The accuracy and operability of this predictive model justify its use to support decision-making processes related to improvement of water productivity in vineyards. This work analyses data obtained on the ground level, while these results are the first step towards applications using other sensors mounted on aerial platforms (e.g. drones or satellites). This is in line with the high number of forthcoming hyperspectral sensors mounted in aerial platforms, which will allow for the generation of hyperspectral time-series, giving access to spatial and temporal dynamics of crop biophysical parameters. Thus, the results presented in this work can be used to support the development of new technologies based on hyperspectral data for vineyards water status monitoring and mapping.

Acknowledgements

I. Pôças acknowledges the Post-Doctoral grant of the project ENGAGE-SKA POCI-01-0145-FEDER-022217, co-funded by FEDER through COMPETE (POCI-01-0145-FEDER-022217). The authors also thank the wine company "Real Companhia Velha" (and its Coordinator for Viticulture, R. Soares) and the wine company "Symington Family Estates" (and its R&D Viticulture Manager, F. Alves) for the facilities provided for fieldwork, as well as the "Associação para o Desenvolvimento da Viticultura Duriense" (ADVID) for funding part of the field-work missions. This study was implemented under a cooperation protocol integrating Faculty of Sciences, University of Porto, ADVID, Real Companhia Velha, and Symington Family Estates.

References

Akaike, H.; 1974: A new look at the statistical model identification. IEEE Transact. Autom. Contr. **19**, 716-723.

Alves, F.; Costa, J.; Costa, P.; Correia, C.; Gonçalves, B.; Soares, R.; Moutinho-Pereira, J.; 2012: Influence of climate and deficit irrigation on grapevine physiology, yield and quality attributes, of the cv. Touriga Nacional at Douro Region, vol. 2, session 7-20. IX[e] Congrès International des Terroirs Vitivinicoles, 25-29 June, 2012. Dijon-Reims, France.

Alves, F.; J, C.; Costa, P.; Correia, C.; Gonçalves, B.; R, S.; Moutinho Pereira, J.; 2013: Grapevine water stress management in Douro Region: Long-term physiology, yield and quality studies in cv. Touriga Nacional. 18[th] Int. Symp. GiESCO 2013, Faculdade de Ciências, Universidade do Porto, Portugal.

Bellvert, J.; Zarco-Tejada, P. J.; Girona, J.; Fereres, E.; 2014: Mapping crop water stress index in a 'Pinot-noir' vineyard: comparing ground measurements with thermal remote sensing imagery from an unmanned aerial vehicle. Precis. Agric. **15**, 361-376.

Blackburn, G. A.; 2007: Hyperspectral remote sensing of plant pigments. J. Exp. Bot. **58**, 855-867.

Blackburn, G. A.; 2010: Spectral indices for estimating photosynthetic pigment concentrations: A test using senescent tree leaves. Int. J. Remote Sens. **19**, 657-675.

Brant, R.; 1990: Assessing Proportionality in the proportional odds model for ordinal logistic regression. Biometrics **46**, 1171-1178.

Brodersen, K. H.; Ong, C. S.; Stephan, K. E.; Buhmann, J. M.; 2010: The balanced accuracy and its posterior distribution, 3121-3124. 20[th] Int. Conf. Pattern Recognition, 23-26 August 2010, Istanbul, Turkey.

Burnham, K. P.; Anderson, D. R.; 2002: Information and likelihood theory: a basis for model selection and inference, 49-97. In: Model selection and multimodel inference: A practical information-theoretic approach, Springer, New York, USA.

Caicedo, J. P. R.; Verrelst, J.; Muñoz-Marí, J.; Moreno, J.; Camps-Valls, G.; 2014: Toward a Semiautomatic Machine Learning Retrieval of Biophysical Parameters. IEEE J. Selec. Topics Appl. Earth Observat. Remote Sens. 7, 1249-1259.

Chaves, M. M.; Zarrouk, O.; Francisco, R.; Costa, J. M.; Santos, T.; Regalado, A. P.; Rodrigues, M. L.; Lopes, C. M.; 2010: Grapevine under deficit irrigation: hints from physiological and molecular data. Ann. Bot. **105**, 661-676.

Clevers, J. G. P. W.; Kooistra, L.; Schaepman, M. E.; 2010: Estimating canopy water content using hyperspectral remote sensing data. Int. J. Appl. Earth Observat. Geoinform. **12**, 119-125.

Coppock, D. L.; 2011: Ranching and multiyear droughts in Utah: Production impacts, risk perceptions, and changes in preparedness. Rangeland Ecol. Manage. **64**, 607-618.

Cunha, M.; Richter, C.; 2016: The impact of climate change on the winegrape vineyards of the Portuguese Douro region. Climat. Change **138**, 239-251.

De Bei, R.; Cozzolino, D.; Sullivan, W.; Cynkar, W.; Fuentes, S.; Dambergs, R.; Pech, J.; Tyerman, S.; 2011: Non-destructive measurement of grapevine water potential using near infrared spectroscopy. Aust. J. Grape Wine Res. **17**, 62-71.

Deloire, A.; Ojeda, H.; Zebic, O.; Bernard, N.; Hunter, J. J.; Carbonneau, A.; 2005: Influence de l'état hydrique de la vigne sur le style de vin. Progr. Agric. Vitic. **122**, 455-462.

Fang, M.; Ju, W.; Zhan, W.; Cheng, T.; Qiu, F.; Wang, J.; 2017: A new spectral similarity water index 505 for the estimation of leaf water content from hyperspectral data of leaves. Remote Sens. Environ. **196**, 13-27.

Feng, S.; Itoh, Y.; Parente, M.; Duarte, M. F.; 2017: Hyperspectral band selection from statistical wavelet models. IEEE Transact. Geosci. Remote Sens. **55**, 2111-2123.

Ferreira, H. A.; 1965: Normais Climatológicas do Continente, Açores e Madeira Correspondentes a 1931-1960. Serviço Meteorológico Nacional, Lisboa, Portugal.

Fox, J.; Weisberg, S.; 2011: An (R) Companion to Applied Regression. Sage Publ, Thousand Oaks (CA), USA.

Gamon, J. A.; Penuelas, J.; Field, C. B.; 1992: A narrow-waveband spectral index that tracks diurnal changes in photosynthetic efficiency. Remote Sens. Environ. **41**, 35-44.

Gitelson, A. A.; Merzlyak, M.; Zur, Y.; Stark, R.; Gritz, U.; 2001a: Non-destructive and remote sensing techniques for estimation of vegetation status, 205-210. Proc. 3[rd] Eur. Conf. Precision Agriculture, Montpelier, France. Grenier & Blackmore, ed.

Gitelson, A. A.; Merzlyak, M. N.; Chivkunova, O. B.; 2001b: Optical properties and nondestructive estimation of anthocyanin content in plant leaves. Photochem. Photobiol. **74**, 38-45.

Harrell, F. E.; 2015: Ordinal Logistic Regression. In: Regression modeling strategies. With applications to linear models, logistic and ordinal regression, and survival analysis, 311-325. Springer International Publ., Cham, Switzerland.

Harrell Jr, F. E.; 2018: rms: Regression Modeling Strategies. R Package Version **5**,1-2.

Huete, A. R.; 1988: A soil-adjusted vegetation index (SAVI). Remote Sens. Environ. **25**, 295-309.

Huete, A. R.; Liu, H. Q.; Batchily, K.; Van Leeuwen, W.; 1997: A comparison of vegetation indices over a global set of TM images for EOS-MODIS. Remote Sens. Environ. **59**, 440-451.

Im, J.; Jensen, J. R.; Coleman, M.; Nelson, E.; 2009: Hyperspectral remote sensing analysis of short 527 rotation woody crops grown with controlled nutrient and irrigation treatments. Geocarto Int. **24**, 293-312.

INMG; 1991: O Clima de Portugal. Fascículo XLIX. Normais Climatológicas da região de Trás-os-Montes e Alto Douro e Beira Interior Correspondentes a 1951-1980, INMG, Lisboa, Portugal.

IVDP; 2018: Instituto dos Vinhos do Douro e Porto, dados Estatísticos sobre a Produção de Vinho do Douro e Porto na Região Demarcada do Douro. Available online at http://www.ivdp.pt/statistics (accessed 27 May 2019).

IVV; 2011: Catálogo das Castas Para Vinho Cultivadas em Portugal. Instituto da Vinha e do Vinho, Lisboa, Portugal.

Jones, G. V.; Alves, F.; 2012: Impact of climate change on wine production: a global overview and regional assessment in the Douro Valley of Portugal. Int. J. Global Warming, **4**, 383-406.

Jones, H. G.; Vaughan, R. A.; 2010: Remote Sensing of Vegetation: Principles, Techniques, and Applications. Oxford University Press Inc., New York, USA.

Kleinbaum, D. G.; Klein, M.; 2010: Ordinal Logistic Regression. In: M. Gail; K. Krickeberg; J. M. Samet; A. Tsiatis; W. Wong (Eds): Logistic Regression. Statistics for Biology and Health. Springer, New York, USA.

Kuhn, M.; 2018: Caret: Classification and Regression Training. R Package Version 6.0-80.

Kuhn, M.; Johnson, K.; 2013: Applied Predictive Modeling. Springer Science+Business Media, New York, USA.

Lehnert, L. W.; Meyer, H.; Bendix, J.; 2017: hsdar: Manage, analyse and simulate hyperspectral data (http://vhrz669.hrz.uni-marburg.de/lcrs/ http://teledetection.ipgp.jussieu.fr/prosail/).

Lopes, C. M.; Santos, T. P.; Monteiro, A.; Rodrigues, M. L.; Costa, J. M.; Chaves, M. M.; 2011: Combining cover cropping with deficit irrigation in a Mediterranean low vigor vineyard. Sci. Hortic. **129**, 603-612.

Maimaitiyiming, M.; Ghulam, A.; Bozzolo, A.; Wilkins, J. L.; Kwasniewski, M. T.; 2017: Early detection of plant physiological responses to different levels of water stress using reflectance spectroscopy. Remote Sens, **9**, 745.

Mariotto, I.; Thenkabail, P. S.; Huete, A.; Slonecker, E. T.; Platonov, A.; 2013: Hyperspectral *versus* multispectral crop-productivity modeling and type discrimination for the HyspIRI mission. Remote Sens. Environ. **139**, 291-305.

McCullagh, P.; 1980: Regression models for ordinal data. Series B (Methodological). J. Royal Statist. Soc. **42**, 109-142.

Medrano, H.; Tomás, M.; Martorell, S.; Escalona, J. M.; Pou, A.; Fuentes, S.; Flexas, J.; Bota, J.; 2015: Improving water use efficiency of vineyards in semi-arid regions. A review. Agron. Sustain. Dev. **35**, 499-517.

Mendiburu, F. D.; 2017: agricolae: Statistical Procedures for Agricultural Research. R Package Version 1.2-3. (http://CRAN.R-project.org/package=agricolae).

Merli, M. C.; Gatti, M.; Galbignani, M.; Bernizzoni, F.; Magnanini, E.; Poni, S.; 2015: Comparison of whole-canopy water use efficiency and vine performance of cv. Sangiovese (*Vitis vinifera* L.) vines subjected to a post-veraison water deficit. Sci. Hortic. **185**, 113-120.

Moutinho-Pereira, J.; Magalhães, N.; Gonçalves, B.; Bacelar, E.; Brito, M.; Correia, C.; 2007: Gas exchange and water relations of three *Vitis vinifera* L. cultivars growing under Mediterranean climate. Photosynthetica **45**, 202-207.

Notario Del Pino, J. S.; Ruiz-Gallardo, J. R.; 2015: Modelling post-fire soil erosion hazard using ordinal logistic regression: A case study in South-eastern Spain. Geomorphology **232**, 117-124.

Oumar, Z.; Mutanga, O.; 2010: Predicting plant water content in *Eucalyptus grandis* forest stands in KwaZulu-Natal, South Africa using field spectra resampled to the Sumbandila Satellite Sensor. Int. J. Appl. Earth Observat. Geoinform. **12**, 158-164.

Peng, C. Y. J.; Lee, K. L.; Ingersoll, G. M.; 2002: An introduction to logistic regression analysis and reporting. J. Educ. Res. **96**, 3-14.

Peñuelas, J.; Filella, I.; Biel, C.; Serrano, L.; Savé, T.; 1993: The reflectance at the 950-970 nm as an indicator of plant water status. I. J. Remote Sens. **14**, 1887-1905.

Peñuelas, J.; Pinol, J.; Ogaya, R.; Filella, I.; 1997: Estimation of plant water concentration by the reflectance Water Index WI (R900/R970). I. J. Remote Sens. **18**, 2869-2875.

Pôças, I.; Gonçalves, J.; Costa, P. M.; Gonçalves, I.; Pereira, L. S.; Cunha, M.; 2017: Hyperspectral-based predictive modelling of grapevine water status in the Portuguese Douro wine region. Int. J. Appl. Earth Observat. Geoinform. **58**, 177-190.

Pôças, I.; Rodrigues, A.; Gonçalves, S.; Costa, P.; Gonçalves, I.; Pereira, L.; Cunha, M.; 2015: Predicting grapevine water status based on hyperspectral reflectance vegetation indices. Remote Sens. **7**, 16460-16479.

Prata-Sena, M.; Castro-Carvalho, B. M.; Nunes, S.; Amaral, B.; Silva, P.; 2018: The terroir of Port wine: Two hundred and sixty years of history. Food Chem, **257**, 388-398.

Qi, J.; Chehbouni, A.; Huete, A. R.; Kerr, Y. H.; Sorooshian, S.; 1994: A modified soil adjusted vegetation index. Remote Sens. Environ. **48**, 119-126.

R Core Team; 2017: R: A Language and Environment for Statistical Computing. R Foundation for Statistical Computing, Vienna, Austria.

Rallo, G.; Minacapilli, M.; Ciraolo, G.; Provenzano, G.; 2014: Detecting crop water status in mature 594 olive groves using vegetation spectral measurements. Biosyst. Engin. **128**, 52-68.

Rivera, J.; Verrelst, J.; Delegido, J.; Veroustraete, F.; Moreno, J.; 2014: On the semi-automatic retrieval of biophysical parameters based on spectral index optimization. Remote Sens. **6**, 4927-4951.

Roberts, D. A.; Roth, K. L.; Perroy, R. L.; 2012: Hyperspectral vegetation indices. In: P. S. Thenkabail, J. G. Lyon, A. Huete (Eds): Hyperspectral remote sensing of vegetation, 309-327. CRC Press. Taylor & Francis Group, Boca Raton, USA.

Rodríguez-Pérez, J. R.; Ordóñez, C.; González-Fernández, A. B.; Sanz-Ablanedo, E.; Valenciano, J. B.; Marcelo, V.; 2018: Leaf water content estimation by functional linear regression of field spectroscopy data. Biosyst. Engin. **165**, 36-46.

Rondeaux, G.; Steven, M.; Baret, F.; 1996: Optimization of soil adjusted vegetation indices. Remote Sens. Environ. **55**, 95-107.

Roujean, J. L.; Breon, F. M.; 1995: Estimating PAR absorbed by vegetation from bidirectional reflectance measurements. Remote Sens. Environ. **51**, 375-384.

Rutherford, G. N.; Guisan, A.; Zimmermann, N. E.; 2007: Evaluating sampling strategies and logistic regression methods for modelling complex land cover changes. J. Appl. Ecol. **44**, 414-424.

Scholander, P. F.; Bradstreet, E. D.; Hemmingsen, E. A.; Hammel, H. T.; 1965: Sap Pressure in Vascular Plants. Negative hydrostatic pressure can be measured in plants. Science **148**, 339-346.

Sonobe, R.; Sano, T.; Horie, H.; 2018: Using spectral reflectance to estimate leaf chlorophyll content of tea with shading treatments. Biosyst. Engin. **175**, 168-182.

Suárez, L.; Zarco-Tejada, P. J.; Sepulcre-Cantó, G.; Pérez-Priego, O.; Miller, J. R.; Jiménez-Muñoz, J. C.; Sobrino, J.; 2008: Assessing canopy PRI for water stress detection with diurnal airborne imagery. Remote Sens. Environ. **112**, 560-575.

Tucker, C. J.; 1979: Red and photographic infrared linear combinations for monitoring vegetation. Remote Sens. Environ. 8, 127-150.

Van Leeuwen, C.; Tregoat, O.; Choné, X.; Bois, B.; Pernet, D.; Gaudillère, J. P.; 2009: Vine water status is a key factor in grape ripening and vintage quality for red Bordeaux wine. How can it be assessed for vineyard management purposes? Oeno One **43**, 798.

Venables, W. N.; Ripley, B. D.; 2002: Modern Applied Statistics with S. 4th Ed. Springer, New York, USA.

Verrelst, J.; Rivera, J.; Alonso, L.; Moreno, J.; 2011: ARTMO: An Automated Radiative Transfer Models Operator toolbox for automated retrieval of biophysical parameters through model inversion. 7th EARSeL SIG-Imag. Spectrosc. Workshop, 11-13 April 2011, Edingburgh, UK.

Verwaeren, J.; Waegeman, W.; De Baets, B.; 2012: Learning partial ordinal class memberships with kernel-based proportional odds models. Comput. Stat. Data Anal. **56**, 928-942.

Wu, C.; Niu, Z.; Tang, Q.; Huang, W.; 2008: Estimating chlorophyll content from hyperspectral vegetation indices: Modeling and validation. Agric. For. Meteorol. **148**, 1230-1241.

Zarco-Tejada, P. J.; González-Dugo, V.; Williams, L. E.; Suárez, L.; Berni, J. a. J.; Goldhamer, D.; Fereres, E.; 2013: A PRI-based water stress index combining structural and chlorophyll effects: Assessment using diurnal narrow-band airborne imagery and the CWSI thermal index. Remote Sens. Environ. **138**, 38-50.

Zarco-Tejada, P. J.; Miller, J. R.; Mohammed, G. H.; Noland, T. L.; Sampson, P. H.; 2002: Vegetation stress detection through chlorophyll + estimation and fluorescence effects on hyperspectral imagery. J. Environ. Qual. **31**, 1433-1441.

Received December 5, 2018
Accepted October 18, 2019